

# Arbovirus-Derived piRNAs Exhibit a Ping-Pong Signature in Mosquito Cells

Nicolas Vodovar<sup>1</sup>, Alfred W. Bronkhorst<sup>2</sup>, Koen W. R. van Cleef<sup>2</sup>, Pascal Miesen<sup>2</sup>, Hervé Blanc<sup>1</sup>, Ronald P. van Rij<sup>2\*</sup>, Maria-Carla Saleh<sup>1\*</sup>

**1** Institut Pasteur, Viruses and RNA interference Group and Centre National de la Recherche Scientifique URA 3015, Paris, France, **2** Department of Medical Microbiology, Radboud University Nijmegen Medical Centre, Nijmegen Centre for Molecular Life Sciences, Nijmegen, The Netherlands

## Abstract

The siRNA pathway is an essential antiviral mechanism in insects. Whether other RNA interference pathways are involved in antiviral defense remains unclear. Here, we report in cells derived from the two main vectors for arboviruses, *Aedes albopictus* and *Aedes aegypti*, the production of viral small RNAs that exhibit the hallmarks of ping-pong derived piwi-associated RNAs (piRNAs) after infection with positive or negative sense RNA viruses. Furthermore, these cells produce endogenous piRNAs that mapped to transposable elements. Our results show that these mosquito cells can initiate *de novo* piRNA production and recapitulate the ping-pong dependent piRNA pathway upon viral infection. The mechanism of viral piRNA production is discussed.

**Citation:** Vodovar N, Bronkhorst AW, van Cleef KWR, Miesen P, Blanc H, et al. (2012) Arbovirus-Derived piRNAs Exhibit a Ping-Pong Signature in Mosquito Cells. PLoS ONE 7(1): e30861. doi:10.1371/journal.pone.0030861

**Editor:** Sebastien Pfeffer, French National Center for Scientific Research - Institut de biologie moléculaire et cellulaire, France

**Received:** October 31, 2011; **Accepted:** December 22, 2011; **Published:** January 24, 2012

**Copyright:** © 2012 Vodovar et al. This is an open-access article distributed under the terms of the Creative Commons Attribution License, which permits unrestricted use, distribution, and reproduction in any medium, provided the original author and source are credited.

**Funding:** This work was financially supported by the French Agence Nationale de la Recherche (ANR-09-394 JJC-0045-01) and the European Research Council (FP7/2007-2013 ERC 242703) to M.C.S., and a VIDI fellowship from the Netherlands Organization for Scientific Research (project number 864.08.003) and Horizon Breakthrough fellowship from the Netherlands Genomics Initiative (project number 93519018) to RPvR. The funders had no role in study design, data collection and analysis, decision to publish, or preparation of the manuscript.

**Competing Interests:** The authors have declared that no competing interests exist.

\* E-mail: r.vanrij@ncmls.ru.nl (RPvR); carla.saleh@pasteur.fr (M-CS)

## Introduction

Arboviruses are maintained in a transmission cycle between hematophagous arthropod vectors and vertebrate hosts. Within their arthropod vector, arboviruses encounter several anatomical and immunological barriers that determine the potential of the virus to be transmitted. RNA interference (RNAi) is a major antiviral defense mechanism in insects [1–8]. A hallmark of the insect antiviral RNAi response is the activation of the pathway by cleavage of viral double-stranded RNA (dsRNA) into 21 nucleotides (nt) viral small interfering RNAs (vsiRNA) by Dicer-2 (Dcr-2). Once produced, vsiRNAs guide the sequence-specific recognition and cleavage of viral target RNAs by an Argonaute-2 (AGO-2) containing RNA induced silencing complex.

The siRNA and piRNA (piwi-interacting RNA) pathways are both gene regulatory mechanisms guided by small silencing RNAs in association with an Argonaute family member. piRNAs differ from siRNAs in several aspects [9]: i) piRNAs are generated in a Dicer-independent manner from single-stranded precursors and display a broader size range of ~25–30 nt; ii) piRNAs associate with the PIWI subclass of the Argonaute family, in flies consisting of piwi, Argonaute-3 (AGO3) and aubergine (aub); iii) PIWI proteins and their associated piRNAs are highly enriched in gonadal tissues, where they protect the germline from activation of transposable elements (TE). Nevertheless, piRNA expression in somatic tissues has recently been reported [10].

Two mechanisms have been proposed for the biogenesis of piRNAs [9]. First, a pool of piRNAs is processed from single-stranded RNA precursors transcribed by chromosomal loci that consist of remnants of TEs. This generates primary piRNAs with a

5' uridine bias ( $U_1$ ) that are usually antisense to TE transcripts. Cleavage of complementary transposon RNA by primary piRNAs initiates the second biogenesis pathway: the ping-pong amplification cycle that involves AGO3 and aub [9]. This amplification loop gives rise to the signature of ping-pong dependent piRNAs: a strong  $U_1$  bias for aub-associated piRNAs and a bias for adenosine at the tenth position ( $A_{10}$ ) of AGO3-associated piRNAs. PIWI-associated piRNAs have a strong strand bias: AGO3 associates with sense TE piRNAs, whereas piwi and aub associate with antisense TE piRNAs [11,12].

While the siRNA pathway is well characterized as an antiviral defense mechanism in insects, the involvement of the piRNA pathway has been recently suggested. Indeed, the potential of the primary piRNA pathway to recognize and process viral RNAs was shown in *Drosophila* ovarian somatic sheet cells (OSS cell line) [13] where in addition to the typical Dcr-2 dependent 21 nt siRNAs, a broader peak of ~25 to 30 nt piRNAs with a  $U_1$  bias was observed. These cells are capable of producing primary piRNAs but are incapable of ping-pong amplification, due to the lack of aub and AGO3 expression [14]. The existence of viral piRNAs has also been suggested in mosquito, but only based on the size range of the viral small RNAs population [15–17].

Here, we show for the first time that mosquito cells infected with (+) and (-) RNA arboviruses produce viral small RNAs with the hallmarks of ping-pong amplification. These results show that mosquito tissue culture faithfully recapitulates the piRNA pathway from an exogenous trigger and may combine RNAi pathways to control a viral infection. These observations have important implications for our understanding of insect innate immunity.

## Results

### Multiple viral small RNAs species in mosquito cells

The C6/36 [18] and U4.4 [19] cell lines were cloned from the same cell population isolated from *Aedes albopictus* larvae [20]. C6/36 cells are devoid of Dcr-2 activity [17], but produce virus-derived small RNA that are longer than vsiRNAs, which were proposed to be viral-derived piRNAs (vpiRNAs) [15,17]. Nevertheless, the absence of functional Dcr-2 activity in C6/36 [17] may have biased these results. To study whether Dcr-2 competent mosquito cells naturally produce vpiRNA, we analyzed viral small RNAs following infection of U4.4 cells. In contrast to C6/36 cells, the U4.4 cells exhibit a functional Dcr-2 activity (Fig. 1). Synthetic <sup>32</sup>P-labelled dsRNA was effectively processed into 21 nt small RNA in U4.4 cell extracts (Fig. 1A), and dsRNA directed against firefly luciferase efficiently silenced plasmid-driven luciferase expression (Fig. 1B). Altogether, these data show that U4.4 cells possess a functional siRNA pathway that should be able to produce vsiRNAs upon virus infection.

To analyze the impact of Dcr-2 activity on the overall virus-derived small RNA population in *A. albopictus* cells, we infected U4.4 cells with Sindbis virus (SINV), a (+) RNA arbovirus, expressing GFP as a reporter of viral replication. Small RNAs ranging from 19 to 30 nt in length were recovered from infected cells and deep sequenced. Consistent with the Dcr-2 activity detected, the size distribution of virus-derived small RNAs displayed a sharp peak at 21 nt (Fig. 1C) that corresponds to vsiRNAs. In addition, a broader Gaussian distribution that peaks at 27–28 nt was observed (Fig. 1C), which has previously also been reported in C6/36 cells [15,17].

### *Aedes albopictus* cells produce vpiRNA through a ping-pong mechanism

We next analyzed the viral small RNA population that peaks at 27–28 nt. Similar to vsiRNAs (Fig. 2A), these small RNAs are distributed across the viral genome, but with an enrichment at the 5' end of the highly expressed SINV-GFP subgenomic RNA (Fig. 2B). They display a strand bias, with more than 69% of the reads mapping to the sense strand of the viral genome.

OSS cells only produced sense primary vpiRNAs that display a strong U<sub>1</sub> bias. In contrast, 25 to 29 nt viral small RNAs from SINV-GFP-infected U4.4 cells originate from both viral RNA strands and display the following nucleotide bias (Fig. 2C): vpiRNAs that mapped on the sense strand exhibit a strong A<sub>10</sub> bias, while vpiRNAs that mapped on the antisense strand displayed a strong U<sub>1</sub> bias. Furthermore, the 5' ends of complementary vpiRNAs are most frequently separated by 10 nt (Fig. 2D), which is characteristic of the ping-pong mechanism for piRNA generation [11]. We therefore propose that these viral small RNAs represent ping-pong derived vpiRNAs.

Viral small RNA profiles from SINV-infected C6/36 cells display a similar profile with a size ranging from 19 to 30 nt [15,17]. We therefore infected C6/36 with SINV-GFP and sequenced the viral small RNA population. Similar to the U4.4 cells, SINV-derived small RNAs from infected C6/36 cells exhibited all the hallmarks of ping-pong amplification (data not shown). Furthermore, the 25–29 nt vpiRNA in C6/36 were resistant to β-elimination, suggesting that they are associated with a PIWI protein and 2' O methylated at their 3' terminal nucleotide (Table 1), similar to piRNAs in *Drosophila* and *Bombyx mori* [21,22]. Altogether, these results show that upon virus infection U4.4 and C6/36 cells produce vpiRNA through a ping-pong amplification mechanism. Furthermore, as C6/36 cells are deficient in Dcr-2

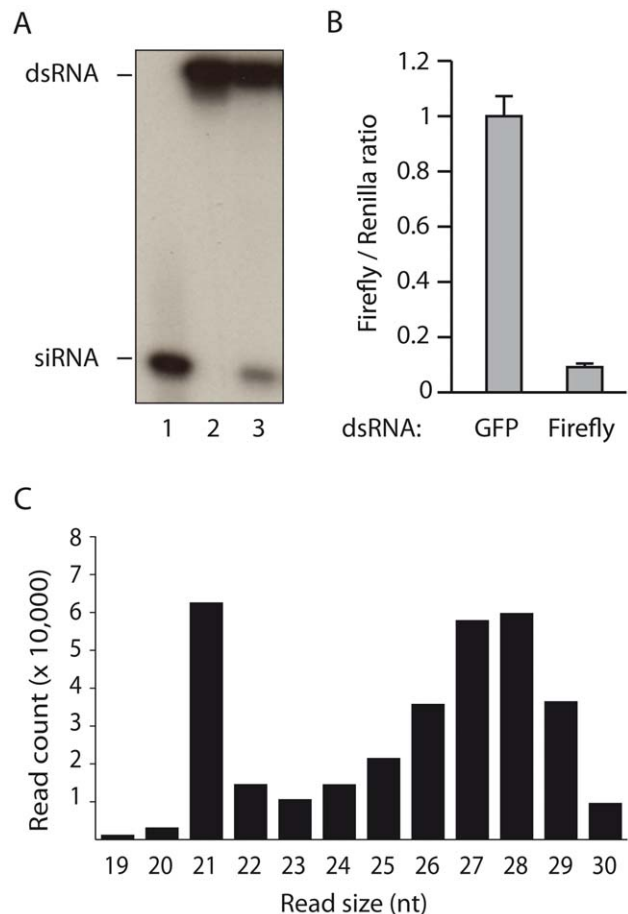


**Figure 1. *Aedes albopictus* U4.4 cells are Dcr-2 competent and produce two populations of viral small RNAs.** **A.** Dicer assay in uninfected U4.4 cells. Lane 3 shows processing of a 113-bp dsRNA substrate into 21-nt siRNAs after incubation in a U4.4 cell extract. Synthetic siRNA (21-nt) and input dsRNA (113-nt) are used as size markers in lanes 1 and 2, respectively. **B.** RNAi reporter assay. Co-transfection of firefly luciferase specific dsRNA with reporter plasmids encoding firefly and *Renilla* luciferase into U4.4 cells results in silencing of the firefly luciferase reporter. GFP dsRNA was used as non-specific dsRNA control. *Renilla* luciferase activity was used as internal control to normalize the firefly luciferase activity. Error bars represent the standard deviations of three individual samples. **C.** Size distribution of the small RNA reads that match the genome of SINV-GFP with 0 mismatches. doi:10.1371/journal.pone.0030861.g001

activity, these results suggest that the piRNA pathway is not a backup mechanism when the antiviral siRNA pathway is defective.

### Ping-pong derived vpiRNAs in (-) RNA virus infection

Given the fundamental differences in replication strategies of (+) and (-) RNA viruses, we next analyzed a published dataset from C6/36 cells infected with La Crosse virus (LACV) [15], an arbovirus with a tri-segmented single-stranded (-) RNA genome [23]. The viral RNA segments serve as templates for transcription of viral mRNAs and for the synthesis of full-length viral complementary RNA. Transcripts from the three segments, Large (L), Medium (M) and Small (S), accumulate at different level (S>M>L) [24]. The absolute number of 25–29 nt virus-derived small RNAs did not follow the differential accumulation of each transcript; however, the number of reads normalized for the length of the segments did mirror the much greater mRNA levels of the S segment [20] (S segment 257.3 reads/nt >>L segment 37.5>M

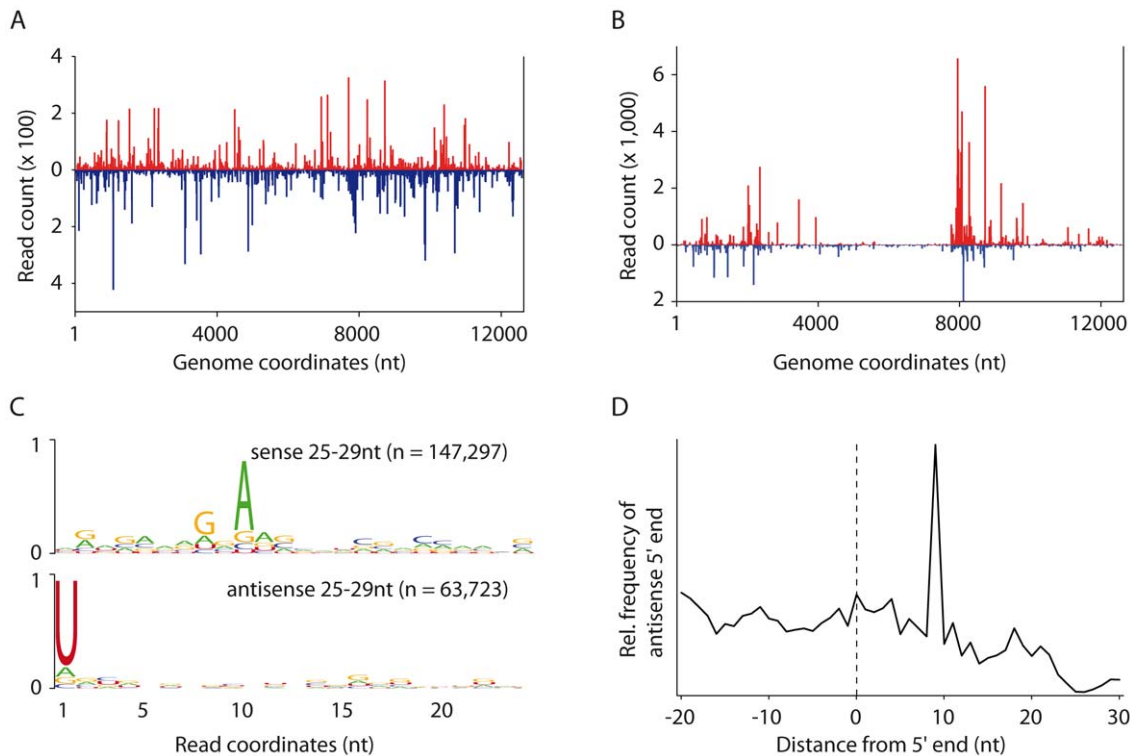


**Figure 2. U4.4 cells produce vsiRNAs and vpiRNAs through a ping-pong mechanism upon (+) ssRNA arbovirus infection.** Profile of 21 nt vsiRNAs (A) and 25–29 nt (B) SINV-GFP-derived small RNAs allowing 0 mismatch during alignment. Viral small RNAs that mapped to the sense and antisense strand of the SINV-GFP genome are shown in red and blue, respectively. C. Conservation and relative nucleotide frequency per position of 25–29 nt SINV-GFP-derived reads that mapped to the sense (top) and the antisense (bottom) strands of the SINV-GFP genome. The overall height of the nucleotide stack indicates the sequence conservation; the height of the nucleotides within each stack represents their relative frequency at that position. n indicates the number of reads used to generate each logo. D. Frequency map of the distance between 25–29 nt small RNAs that mapped to opposite strands of the SINV-GFP genome. The peak at position 9 on the sequence (the first nucleotide being position 0) indicates the position of maximal probability of finding the 5' end of a complementary small RNA. doi:10.1371/journal.pone.0030861.g002

segment 19.5). The relative amounts of vpiRNA mapping on each strand of the viral segments differed among the three segments, with ratios of sense over antisense vpiRNAs of 20.3, 4.3, and 0.7 for S, M and L, respectively (Fig. 3A–C). This strand bias of vpiRNA followed the previously estimated gradient of mRNA over viral genome ratios from highly (S) to lower (L) expressed transcripts [20].

Analysis of the nucleotide biases indicated that all segments presented a U<sub>1</sub> bias on the genomic (–) strand and an A<sub>10</sub> bias for the antigenomic (+) RNA strand (Fig. 3A–C). In addition, complementary vpiRNAs are enriched for those in which the 5' ends are separated by exactly 10 nucleotides (Fig. 3D–F). Thus similar to the (+) RNA virus SINV, LACV viral RNAs are targets

for ping-pong dependent vpiRNA biogenesis with U<sub>1</sub> vpiRNAs originating from the negative strand, regardless of viral genome polarity and relative abundance of transcript.

### *Aedes aegypti* Aag2 cells produce vsiRNA and vpiRNA with a ping-pong signature

*A. albopictus* and *A. aegypti* are the major vectors for arboviruses within the *Aedes* genus of culicine mosquitoes. To test whether vpiRNA production also occurs in cells from *A. aegypti*, we analyzed small RNAs in the Aag2 cell line [25] after infection with SINV-GFP.

We observed a size distribution of virus-derived small RNAs with a sharp peak at 21 nt and a broader Gaussian distribution that peaks at 28 nt (Fig. 4A). Similar to previous observations of Alphavirus infected Aag2 cells [26], the 21 nt vsiRNAs mapped across the viral genome in similar proportions over viral sense and antisense strands (Fig. 4B). The viral small RNAs of 25 to 29 nt are distributed across the viral genome, but enriched at the 5' end of the highly expressed SINV subgenomic RNA (Fig. 4C). Furthermore, these small RNAs display the hallmarks of ping-pong dependent piRNAs (Fig. 4D–E) as observed in *A. albopictus* cells. Together, our results show that three different cell lines derived from the two major mosquito vectors for arboviruses have a functional PIWI pathway and produce ping-pong derived piRNAs after infection with Sindbis virus.

The PIWI gene family has greatly expanded in *A. aegypti*. In addition to a single *Ago3* orthologue, the *A. aegypti* genome encodes

**Table 1. vpiRNAs are resistant to beta-elimination.**

	C6/36 + SINV-GFP	
	No treatment	Beta-elimination
Total number of reads* (19-29nt)	916,504	1,028,574
miRNA reads* (22nt)	286,711	146,225
25–29 nt viral reads	23,737	242,762

\*Numbers of reads matching the *Drosophila melanogaster* genome available at flybase and miRNA sequences available at mirBase. doi:10.1371/journal.pone.0030861.t001

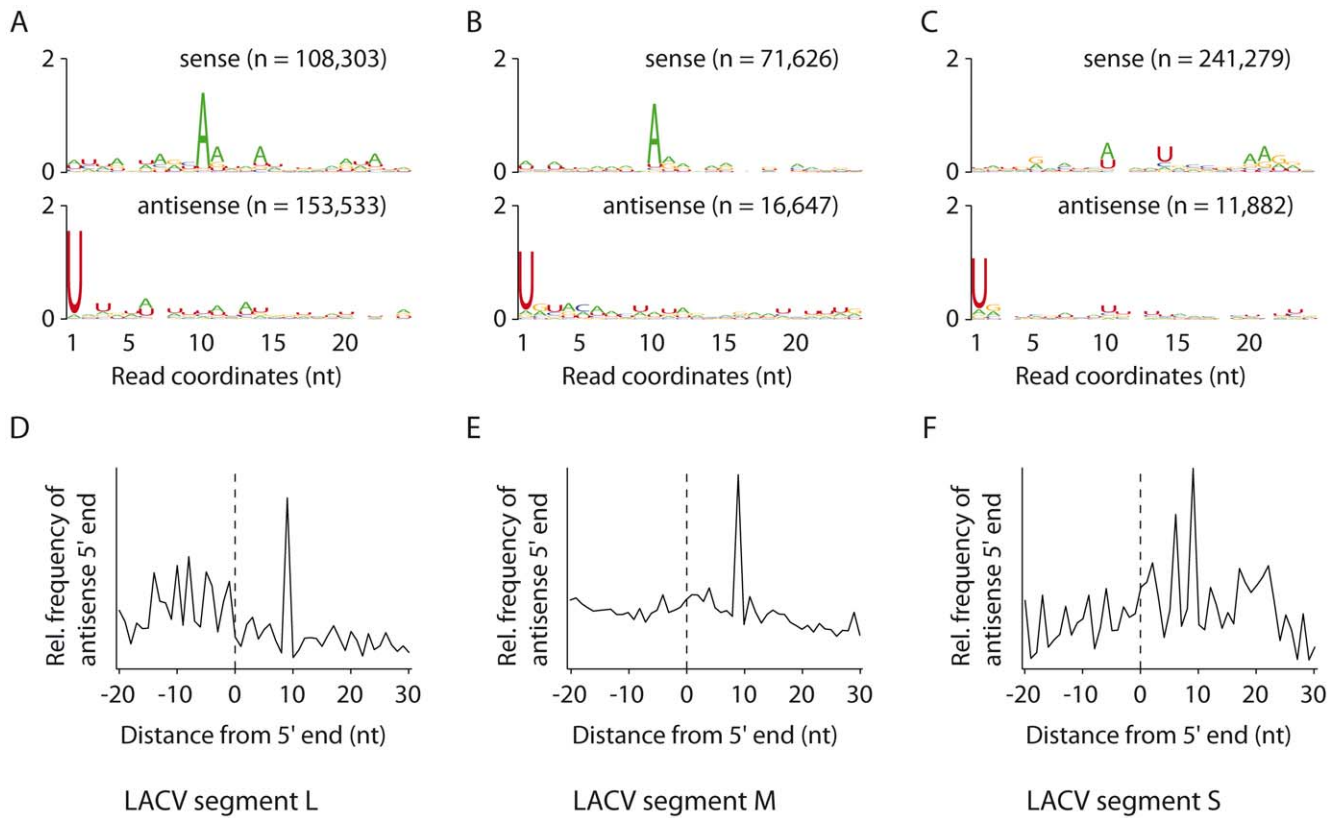


**Figure 3. *Aedes albopictus* C6/36 cells produce ping-pong dependent vpiRNA upon (-) RNA virus infection. A, B, and C.** Conservation and relative nucleotide frequency per position of the 25–29 nt LACV-derived reads that mapped to the antigenomic sense (top) and genomic antisense (bottom) strands of the LACV genome segments L, M and S, respectively. n indicates the number of reads used to generate each logo. **D, E, and F.** Frequency map of the distance between 25–29 nt reads that mapped to opposite strands of the LACV genome segments L, M and S, respectively. The peak at position 9 on the sequence (the first nucleotide being position 0) indicates the position of maximal probability of finding the 5' end of a complementary small RNA.  
doi:10.1371/journal.pone.0030861.g003

seven *Piwi/Aub* orthologues [27]. Based on their clustering with *Anopheles gambiae* *Ago4* and *Ago5*, *A. aegypti* *Piwi1* through *Piwi4* belong to the *Ago4* clade, whereas *Piwi5* to *Piwi7* belong to the *Ago5* clade. Our observation of ping-pong derived vpiRNAs in mosquito cells implies that PIWI proteins from the different clades are expressed in these cells. Indeed, we readily detected in Aag2 cells transcripts from multiple PIWI family members, including *Piwi4*, *Piwi5*, *Piwi6*, and *Ago3* (Fig. 4F).

To address a potential germline source of the Aag2 cells, we analyzed the expression of *Nanos* in Aag2 cells, but we were unable to detect any transcripts by RT-PCR (data not shown). While this result does not rule out a germline origin of the cell line, we do note that the identification of piRNAs with a ping-pong signature in somatic tissues in flies implies that a functional PIWI pathway is present in the soma of insects [10].

### *Aedes aegypti* Aag2 cells produce transposon-derived piRNAs with a ping-pong signature

Our results imply that the piRNA pathway targets replicating RNA viruses in mosquito cells. The majority of piRNAs in *Drosophila* and other animals were described to map to transposable elements. As the genome sequence of *A. aegypti* is available [28], we analyzed whether Aag2 cells engage in ping-pong dependent amplification of TE derived piRNAs. We mapped the non-viral small RNAs to a dataset that contain full-length non-composite transposons sequences (<http://tefam.biochem.vt.edu/>

<http://tefam/index.php>). TE-derived small RNAs display a sharp 21 nt peak and a broader peak centering around 27 nt, which is suggestive of TE targeting by the *Aedes* siRNA and piRNA pathways (Fig. 5A). In contrast to TE-derived endo-siRNAs, the vast majority of TE piRNAs derive from retrotransposons and not from DNA transposons (Fig. 5A). For most retrotransposons, the 25–29 nt TE RNAs display a strong over-representation of antisense reads (Fig. 5B–C). The sequence depth of our library did not allow us to analyze ping-pong signatures in individual TEs. We therefore analyzed sequence logos of 25–29 nt small RNAs of the entire retrotransposon dataset (Fig. 5D). A strong U<sub>1</sub> bias for antisense small RNAs and an enrichment of A<sub>10</sub> in sense small RNAs imply that, similar to *Drosophila*, TEs are processed by the piRNA pathway in a ping-pong dependent manner in Aag2 cells.

### Discussion

Antiviral RNAi activity in insects has thus far only been attributed to the siRNA pathway. The identification of vpiRNAs in *Drosophila* OSS cells [13] and in *A. aegypti* and *A. albopictus* cells (this study) strongly suggests that the piRNA pathway constitutes another facet of the antiviral RNAi response in insects. Unlike the siRNA pathway, the piRNA pathway is highly enriched in the gonads where it plays a critical role in the control of transposition in the germ line. Because arboviruses can be transmitted vertically in arthropod vectors [29], an antiviral piRNA response in the gonads may constitute an antiviral mechanism to limit vertical



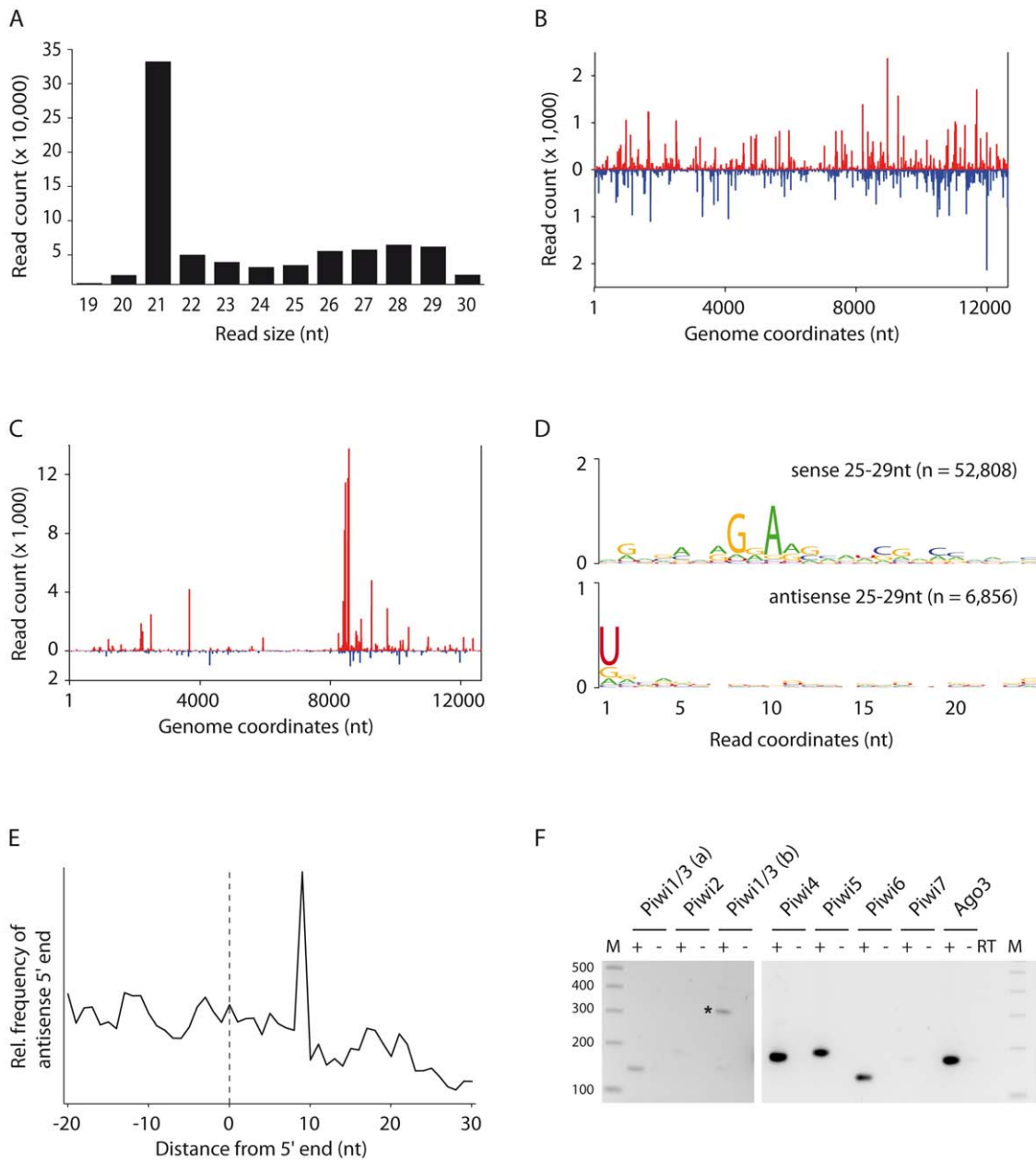


**Figure 4. *Aedes aegypti* Aag2 cells produce vsRNA and vpiRNA with a ping-pong signature upon arbovirus infection.** **A.** Size distribution of the small RNA reads that match the genome of SINV-GFP with 0 mismatches. Profile of 21 nt vsRNAs (**B**) and 25–29 nt (**C**) SINV-GFP-derived small RNAs allowing 0 mismatch during alignment. Viral small RNA that mapped to the sense and antisense strand of the SINV-GFP genome are shown in red and blue, respectively. **D.** Conservation and relative nucleotide frequency per position of 25–29 nt SINV-GFP-derived reads that mapped to the sense (top) and antisense (bottom) strands of the SINV-GFP genome. n indicates the number of reads used to generate each logo. **E.** Frequency map of the distance between 25–29 nt small RNAs that mapped to opposite strands of the SINV-GFP genome. The peak at position 9 on the sequence (the first nucleotide being position 0) indicates the position of maximal probability of finding the 5' end of a complementary small RNA. **F.** Expression of PIWI family members in Aag2 cells analyzed by RT-PCR. cDNA synthesis was performed in the presence (+) or absence (–) of reverse transcriptase (RT). The –RT samples are included as controls for contamination of RNA preparations with chromosomal DNA. The coding sequences of Piwi1 and Piwi3 are 95% identical at the nucleotide level. Two different primer sets that amplify both Piwi1 and Piwi3 were used (a and b). A higher exposure was used for the gel image with Piwi1 to Piwi3. A 100 bp ladder was used as a size marker (M). The asterisk indicates a non-specific PCR amplification product.

doi:10.1371/journal.pone.0030861.g004

transmission of arboviruses in insect vectors. In addition, a putative somatic piRNA pathway may represent an important aspect of vector competence. While the relevance of the piRNA pathway in controlling virus infections awaits experimental validation, it is likely that a pathway that efficiently cleaves viral RNA affects virus replication. Hence, the piRNA pathway should

be considered as an intrinsic component of the antiviral RNAi response in insects. Moreover, U4.4 and Aag2 cells emerge as an attractive model to dissect piRNA biogenesis and the interplay between siRNA and piRNA pathways.

Contrary to the OSS cell line that only produces primary vpiRNAs [13], U4.4, Aag2 and C6/36 cells produce primary and

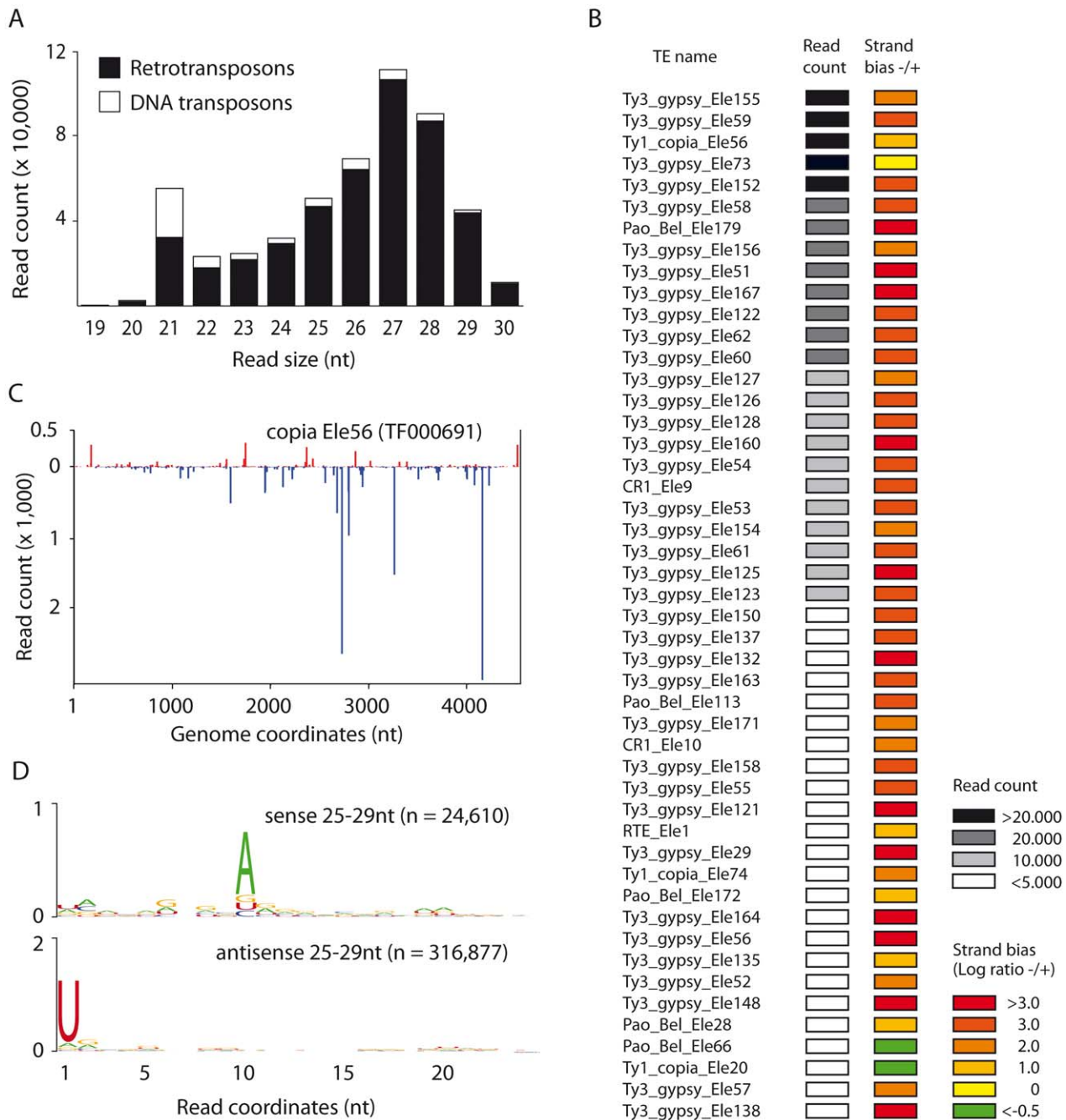


**Figure 5. *Aedes aegypti* Aag2 cells produce transposon-derived piRNAs with a ping-pong signature.** **A.** Size distribution of the small RNA reads that match with 0 mismatches against an *Aedes aegypti* transposon dataset that contain full-length non-composite transposon sequences (TEfam: <http://tefam.biochem.vt.edu/tefam/index.php>). **B.** Heat map for 25–29 nt small RNAs that mapped to individual retrotransposons with more than 1000 reads. Read count and log-transformed ratios of antisense/sense small RNAs are presented. **C.** Profile of 25–29 nt reads that mapped to the transposon Copia Ele56 (TF000691) allowing 0 mismatch during alignment. Transposon-derived piRNAs that mapped to the sense and antisense strand of the transposon sequence are shown in red and blue, respectively. **D.** Conservation and relative nucleotide frequency per position of 25–29 nt reads that mapped to the sense (top) and the antisense (bottom) strands of the entire transposon dataset. n indicates the number of reads used to generate each logo. doi:10.1371/journal.pone.0030861.g005

secondary vpiRNAs through a ping-pong mechanism. In OSS cells, vpiRNAs map predominantly to the positive strand of the genome of (+) RNA viruses and display the expected  $U_1$  bias for primary piRNAs. In U4.4, Aag-2 and C6/36 cells however, the nucleotide bias signature is inverted, regardless the polarity of the viral genome. The vpiRNAs that derive from the (–) strand (i.e. the antigenomic strand of SINV and the genomic RNA strand of LACV) present a

$U_1$  bias, whereas those that derive from the (+) strand display an  $A_{10}$  bias. This disparity between OSS cells and mosquito cells is unlikely to be due to differences in piRNA biogenesis, as our results on TE piRNAs in Aag-2 and observations in *Bombyx Mori* BmN4 cells [30] suggest that basic features of piRNA biogenesis are conserved among insects. It is then most likely that this inversion is based on intrinsic features of the viral lifecycle.

The +/− strand ratio is uneven in ssRNA viruses. In (+) RNA viruses, the (+) strand is over-represented compared to the negative strand that serves as template for the production of progeny viral RNA. In many (−) RNA viruses, the (+) viral RNA strand that corresponds to viral transcript is over-represented compared to the genomic (−) strand, although the relative amounts of transcripts are variable. In LACV, there is a gradient of +/− strand ratio between highly (S segment) and slightly (L segment) expressed transcripts. In both (+) and (−) RNA viruses, the genome and the intermediates of replication are shielded from cytoplasmic components, contrary to viral RNAs that engage in translation. Interestingly, primary vpiRNAs are produced from the (−) strand, regardless viral genome polarity. Moreover, in most cases, the ratio between U<sub>1</sub> and secondary A<sub>10</sub> vpiRNAs follows strand stoichiometry. According to these observations, we propose two non-mutually exclusive hypotheses for the production of vpiRNAs through a ping-pong mechanism. The first hypothesis is based on the relative amounts of (+) and (−) strands during viral replication. For primary vpiRNAs that are produced from the abundant (+) strand, the generation of secondary vpiRNAs from the (−) strand is limited due to the relative limited amount of viral (−) RNA strands. Conversely, the production of primary vpiRNAs from the (−) strand may allow the generation of abundant secondary vpiRNAs from the abundant (+) strand. According to this hypothesis, as the (+) strand is more abundant than the (−) strand, the second ping-pong mechanism supersedes the first one. As a second hypothesis, the production of primary vpiRNAs from the (−) strand may result for a differential accessibility of the viral RNAs by piRNA pathway components. We propose that the PIWI protein that is responsible for primary piRNA biogenesis can better access viral (−) RNAs, and that the PIWI proteins that are responsible for secondary piRNA biogenesis can mostly access viral (+) RNAs. This may be due to spatial restriction of piRNA pathway proteins or to a differential accessibility of PIWI proteins to the viral RNAs engaged in replication and in translation.

Finally, we show that viruses trigger the piRNA and the siRNA pathways in a similar way as transposons. This suggests that the RNAi pathways only discriminate common features of parasitic nucleic acids rather than their origin.

## Materials and Methods

### Cell culture, virus production and infection

*A. albopictus* U4.4 cells and *A. aegypti* Aag2 cells ([19,25], kindly provided by G.P. Pijlman, Wageningen University, the Netherlands) were cultured at 28°C in Leibovitz L-15 medium (Invitrogen) supplemented with 10% heat inactivated fetal calf serum (FCS, Invitrogen), 2% Tryptose Phosphate Broth Solution (Sigma) and 1% Non-Essential Amino Acids (Invitrogen). BHK-21 cells (American Type Culture Collection) were cultured in DMEM medium (Invitrogen) supplemented with 10% FCS (Invitrogen), and maintained at 37°C in 5% CO<sub>2</sub>. *In vitro* transcribed RNA from recombinant SINV expressing the Green Fluorescent Protein [31] was transfected into BHK-21 cells. Virus titer was determined by plaque assay on BHK-21 cells. 2 × 10<sup>6</sup> U4.4 were infected with SINV-GFP for 2 hours in culture medium at a multiplicity of

infection of 1. Cells were harvested 2 days post-infection, when 80–90% of the cells were positive for GFP expression.

### RNAi reporter and Dicer assays

RNAi reporter assays were adapted from [32], using 3 × 10<sup>5</sup> U4.4 cells per well of a 24-well plate, 156 ng of pMT-Luc and pMT-Ren plasmids [6], and 0.625 ng of either firefly luciferase or GFP dsRNA. Dicer activity was determined in cell extracts from uninfected U4.4 cells as previously described [33], using 100 counts per seconds of a uniformly <sup>32</sup>P-radiolabeled 113-bp dsRNA substrate.

### Small RNA library preparation and analysis

Small RNA libraries were prepared as described [34] and sequenced on a Genome Analyzer *Iix* (Illumina). Virus-derived small RNAs were analyzed using Papparazzi [35]. piRNA signatures were calculated using in-house Perl scripts from 25–29 nucleotide-long virus-derived small RNA as previously described [11]. Nucleotide frequencies per position were displayed using the WebLogo program [36]. 19–30 nt reads from the Aag2 small RNA library were aligned with 0 mismatch against the *Aedes aegypti* transposon dataset available at Tefam (<http://tefam.biochem.vt.edu/tefam/>). The aligned reads were processed similarly to the virus-derived small RNA with in-house Perl scripts. Sequences were submitted to the Sequence Read Archive at the National Center for Biotechnology Information under accession number SRA047263.

### RT-PCR

Total RNA was isolated from a confluent 75 cm<sup>2</sup> flask of Aag2 cells using Isol-RNA Lysis Reagent (5 Prime) according to manufacturer's recommendations. cDNA synthesis was performed on 1 µg of DNase-I (Invitrogen) treated total RNA using an oligo-dT primer and TaqMan reverse transcriptase (Roche). PCR was performed using the following primers: F-AaeNanos, CAAACGT-GAAGCGGAAGATT; R-AaeNanos, AATCAACGATGGAT-CGGATT; F-AaePIWI1/3a, TGTAGGGGAAGTAATGCA-TCCG; R-AaePIWI1/3a, TCTACGGCAATGGTATCTGCT; F-AaePIWI1/3b, GGCCGTTAGCGAGTCTCAT; R-AaePIWI1/3b, GGCAGAACCTTCGTGGTAAG; F-AaePIWI2, ATGAA-AGCCGGAAGGTC; R-AaePIWI2, CTGCTACCATTGCCA-TTTC; F-AaePIWI4, TGACCGTTACTCTCAAGGCGC-TACCGT; R-AaePIWI4, GACCGTTCACGGCCACCTGCC-GAT; F-AaePIWI5, GCCATACATCGGGTCAAAT; R-AaePIWI5, TGAGGTTGTTGCTTCTGAGGT; F-AaePIWI6, TA-ATCCACAGGAAGGCTCCA; R-AaePIWI6, CTCCTCCA-TTGTCCGATCCT; F-AaePIWI7, GGAGGTTCGTGGAGG-TAACAA; R-AaePIWI7, CCTTCCAATCAGGATTGCTT; F-AaeAgo3, TCGGTTTACCGCCAGCTGGGAGTTTTG; R-AaeAgo3, AGGTTATCTCAGCGGGAAAATCATGTGCT.

### Author Contributions

Conceived and designed the experiments: RPvR M-CS. Performed the experiments: AWB KWRvC PM HB. Analyzed the data: NV RPvR M-CS. Wrote the paper: NV RPvR M-CS. Contributed bioinformatics tools: NV.

## References

- Campbell CL, Keene KM, Brackney DE, Olson KE, Blair CD, et al. (2008) *Aedes aegypti* uses RNA interference in defense against Sindbis virus infection. *BMC Microbiol* 8: 47.
- Galiana-Arnoux D, Dostert C, Schneemann A, Hoffmann JA, Imler JL (2006) Essential function in vivo for Dicer-2 in host defense against RNA viruses in drosophila. *Nat Immunol* 7: 590–597.
- Keene KM, Foy BD, Sanchez-Vargas I, Beaty BJ, Blair CD, et al. (2004) RNA interference acts as a natural antiviral response to O'nyong-nyong virus (Alphavirus; Togaviridae) infection of *Anopheles gambiae*. *Proc Natl Acad Sci U S A* 101: 17240–17245.
- Myles KM, Wiley MR, Morazzani EM, Adelman ZN (2008) Alphavirus-derived small RNAs modulate pathogenesis in disease vector mosquitoes. *Proc Natl Acad Sci U S A* 105: 19938–19943.
- Sanchez-Vargas I, Scott JC, Poole-Smith BK, Franz AW, Barbosa-Solomieu V, et al. (2009) Dengue virus type 2 infections of *Aedes aegypti* are modulated by the mosquito's RNA interference pathway. *PLoS Pathog* 5: e1000299.

6. van Rij RP, Saleh MC, Berry B, Foo C, Houk A, et al. (2006) The RNA silencing endonuclease Argonaute 2 mediates specific antiviral immunity in *Drosophila melanogaster*. *Genes Dev* 20: 2985–2995.
7. Wang XH, Aliyari R, Li WX, Li HW, Kim K, et al. (2006) RNA interference directs innate immunity against viruses in adult *Drosophila*. *Science* 312: 452–454.
8. Zamboni RA, Vakharia VN, Wu LP (2006) RNAi is an antiviral immune response against a dsRNA virus in *Drosophila melanogaster*. *Cell Microbiol* 8: 880–889.
9. Siomi MC, Sato K, Pezic D, Aravin AA (2011) PIWI-interacting small RNAs: the vanguard of genome defence. *Nat Rev Mol Cell Biol* 12: 246–258.
10. Yan Z, Hu HY, Jiang X, Maierhofer V, Neb E, et al. (2011) Widespread expression of piRNA-like molecules in somatic tissues. *Nucleic Acids Res* 39: 6596–6607.
11. Brennecke J, Aravin AA, Stark A, Dus M, Kellis M, et al. (2007) Discrete small RNA-generating loci as master regulators of transposon activity in *Drosophila*. *Cell* 128: 1089–1103.
12. Gunawardane LS, Saito K, Nishida KM, Miyoshi K, Kawamura Y, et al. (2007) A slicer-mediated mechanism for repeat-associated siRNA 5' end formation in *Drosophila*. *Science* 315: 1587–1590.
13. Wu Q, Luo Y, Lu R, Lau N, Lai EC, et al. (2010) Virus discovery by deep sequencing and assembly of virus-derived small silencing RNAs. *Proc Natl Acad Sci U S A* 107: 1606–1611.
14. Lau NC, Robine N, Martin R, Chung WJ, Niki Y, et al. (2009) Abundant primary piRNAs, endo-siRNAs, and microRNAs in a *Drosophila* ovary cell line. *Genome Res* 19: 1776–1785.
15. Brackney DE, Scott JC, Sagawa F, Woodward JE, Miller NA, et al. (2010) C6/36 *Aedes albopictus* cells have a dysfunctional antiviral RNA interference response. *PLoS Negl Trop Dis* 4: e856.
16. Hess AM, Prasad AN, Pütsyn A, Ebel GD, Olson KE, et al. (2011) Small RNA profiling of Dengue virus-mosquito interactions implicates the PIWI RNA pathway in anti-viral defense. *BMC Microbiol* 11: 45.
17. Scott JC, Brackney DE, Campbell CL, Bondu-Hawkins V, Hjelle B, et al. (2010) Comparison of dengue virus type 2-specific small RNAs from RNA interference-competent and -incompetent mosquito cells. *PLoS Negl Trop Dis* 4: e848.
18. Igarashi A (1978) Isolation of a Singh's *Aedes albopictus* cell clone sensitive to Dengue and Chikungunya viruses. *J Gen Virol* 40: 531–544.
19. Condreay LD, Brown DT (1986) Exclusion of superinfecting homologous virus by Sindbis virus-infected *Aedes albopictus* (mosquito) cells. *J Virol* 58: 81–86.
20. Singh KPR (1967) Cell cultures derived from larvae of *Aedes albopictus* (Skuse) and *Aedes aegypti* (L.). *Curr Sci* 36: 56–508.
21. Kawaoka S, Izumi N, Katsuma S, Tomari Y (2011) 3' End Formation of PIWI-Interacting RNAs In Vitro. *Molecular Cell* 43: 1015–1022.
22. Horwich MD, Li CJ, Matraga C, Vagin V, Farley G, et al. (2007) The *Drosophila* RNA methyltransferase, DmHen1, modifies germline piRNAs and single-stranded siRNAs in RISC. *Current Biology* 17: 1265–1272.
23. Borucki MK, Kempf BJ, Blitvich BJ, Blair CD, Beaty BJ (2002) La Crosse virus: replication in vertebrate and invertebrate hosts. *Microbes and Infection* 4: 341–350.
24. Rossier C, Raju R, Kolakofsky D (1988) LaCrosse virus gene expression in mammalian and mosquito cells. *Virology* 165: 539–548.
25. Peleg J (1968) Growth of Arboviruses in Monolayers from Subcultured Mosquito Embryo Cells. *Virology* 35: 617–8.
26. Siu RWC, Fragkoudis R, Simmonds P, Donald CL, Chase-Topping ME, et al. (2011) Antiviral RNA Interference Responses Induced by Semliki Forest Virus Infection of Mosquito Cells: Characterization, Origin, and Frequency-Dependent Functions of Virus-Derived Small Interfering RNAs. *Journal of Virology* 85: 2907–2917.
27. Campbell CL, Black WC, Hess AM, Foy BD (2008) Comparative genomics of small RNA regulatory pathway components in vector mosquitoes. *Bmc Genomics* 9.
28. Nene V, Wortman JR, Lawson D, Haas B, Kodira C, et al. (2007) Genome sequence of *Aedes aegypti*, a major arbovirus vector. *Science* 316: 1718–1723.
29. Hanley KA, Weaver SC (2008) Arbovirus Evolution. In: Domingo E, Parrish CR, Holland JJ, eds. *Origin and evolution of viruses*. St. Louis: MO: Elsevier. pp 351–392.
30. Kawaoka S, Hayashi N, Suzuki Y, Abe H, Sugano S, et al. (2009) The Bombyx ovary-derived cell line endogenously expresses PIWI/PIWI-interacting RNA complexes. *RNA* 15: 1258–1264.
31. Saleh MC, Tassetto M, van Rij RP, Goic B, Gausson V, et al. (2009) Antiviral immunity in *Drosophila* requires systemic RNA interference spread. *Nature* 458: 346–350.
32. van Cleef KW, van Mierlo JT, van den Beek M, van Rij RP (2011) Identification of viral suppressors of RNAi by a reporter assay in *Drosophila* S2 cell culture. *Methods Mol Biol* 721: 201–213.
33. Haley B, Tang G, Zamore PD (2003) In vitro analysis of RNA interference in *Drosophila melanogaster*. *Methods* 30: 330–336.
34. Gausson V, Saleh MC (2011) Viral small RNA cloning and sequencing. *Methods Mol Biol* 721: 107–122.
35. Vodovar N, Goic B, Blanc H, Saleh MC (2011) In silico reconstruction of viral genomes from small RNAs improves viral-derived siRNA profiling. *J Virol*.
36. Crooks GE, Hon G, Chandonia JM, Brenner SE (2004) WebLogo: a sequence logo generator. *Genome Res* 14: 1188–1190.